Saudi Journal of Biological Sciences (2017) **24**, 548–555

King Saud University

Saudi Journal of Biological Sciences

www.ksu.edu.sa
www.sciencedirect.com

ORIGINAL ARTICLE

The research of constructing dynamic cognition model based on brain network

Fang Chunying [a,b], **Li Haifeng** [a,*], **Ma Lin** [a]

[a] *School of Computer Science and Technology, Harbin Institute of Technology, 150001 Harbin, China*
[b] *School of Computer and Information Engineering, Heilongjiang University of Science and Technology, 150027 Harbin, China*

Received 26 October 2016; revised 5 January 2017; accepted 9 January 2017
Available online 24 January 2017

KEYWORDS

Wavelet coherence;
Brain functional connectivity;
Dynamic evolution model;
Cognition process

Abstract Estimating the functional interactions and connections between brain regions to corresponding process in cognitive, behavioral and psychiatric domains is a central pursuit for understanding the human connectome. Few studies have examined the effects of dynamic evolution on cognitive processing and brain activation using brain network model in scalp electroencephalography (EEG) data. Aim of this study was to investigate the brain functional connectivity and construct dynamic programing model from EEG data and to evaluate a possible correlation between topological characteristics of the brain connectivity and cognitive evolution processing. Here, functional connectivity between brain regions is defined as the statistical dependence between EEG signals in different brain areas and is typically determined by calculating the relationship between regional time series using wavelet coherence. We present an accelerated dynamic programing algorithm to construct dynamic cognitive model that we found that spatially distributed regions coherence connection difference, the topologic characteristics with which they can transfer information, producing temporary network states. Our findings suggest that brain dynamics give rise to variations in complex network properties over time after variation audio stimulation, dynamic programing model gives the dynamic evolution processing at different time and frequency. In this paper, by applying a new construct approach to understand whole brain network dynamics, firstly, brain network is constructed by wavelet coherence, secondly, different time active brain regions are selected by network topological characteristics and minimum spanning tree. Finally, dynamic evolution model is constructed to understand cognitive process by dynamic programing algorithm, this model is applied to the auditory experiment, results showed that, quantitatively, more correlation was

* Corresponding author.
E-mail addresses: fcy3333@163.com (F. Chunying), Lihaifeng@hit.edu.cn (L. Haifeng), malin_li@hit.edu.cn (M. Lin).
Peer review under responsibility of King Saud University.

Production and hosting by Elsevier

http://dx.doi.org/10.1016/j.sjbs.2017.01.025

observed after variation audio stimulation, the EEG function connection dynamic evolution model on cognitive processing is feasible with wavelet coherence EEG recording.

1. Introduction

Brain functional connectivity has played a variety of roles in the study of human cognition and behavior over the past four decades. Functional connectivity has revealed the reorganization of brain networks during cognitive tasks (Sporns, 2011). Thus, in this paper, dynamic evolution model is constructed to understand cognitive process by dynamic programing algorithm based on brain network. Initially, computed tomography (CT) and then magnetic resonance imaging (MRI) were used to probe the large-scale organization of the brain which is estimated by correlation of BOLD activity, identifies coherent brain activity in distributed and reproducible networks (Vincent et al., 2006). More recently, a variety of imaging modalities—including structural and functional MRI and positron emission tomography (PET) studies have shown characteristic changes in the brains, but thus far has been limited in its capacity to study their temporal evolution. Therefore, the purpose of this paper is to present a data-driven dynamic construction of the state space for the one-pass dynamic programming algorithm so that only the actually active hypotheses are explicitly generated during the process of cognition.

A fair amount of investigation has been directed at linking spiking activity to the fMRI blood oxygenation level-dependent (BOLD) response (Nagai et al., 2004), but far less research has sought to relate spiking activity and EEG. The EEG is thought to reflect the postsynaptic potentials in the apical dendrites of pyramidal cells resulting from their mutual alignment, which allows summation of electric fields (Kopal and Burian, 2014). The strength of the signal is related to both the magnitude of the postsynaptic activity and its coherence: postsynaptic currents with low spatiotemporal coherence tend to destructively interfere at the level of the scalp (Lachaux et al., 2002; Onnela et al., 2005). The common synaptic activity that drives variability in the EEG signal likely also generates spike count correlation across neurons. Their cortical generator was calculated using wavelet coherence for each group. Coherence analysis has been extensively applied to the study of neural activity. To overcome the problems due to non-stationary raised in the previous section, it has recently been proposed to apply wavelet analysis for the estimation of coherence among non-stationary signals (Milligen et al., 1995; Santoso et al., 1997). In contrast to Fourier analysis, wavelet analysis has been devised to analyze signals with rapidly changing spectra (Torrence and Compo, 1998). It performs what is called a time–frequency analysis of the signal, which means the estimation of the spectral characteristics of the signal as a function of time. In some sense, wavelet analysis is close to the windowed short-term Fourier transform, especially when using the Morlet wavelet (Osofsky, 2000), but the major difference is that the size of the window is fixed for the short-term Fourier, and it is adapted to the frequency of the signal in wavelet analysis. Because of this difference, wavelet analysis has a more accurate time–frequency resolution (Lachaux et al., 2000; Bonato et al., 1996). However, the utility of wavelet analysis is that it provides not only the time-varying power-spectrum, but also the phase spectrum, which is needed to compute the coherence. This makes wavelet analysis a natural choice for the estimation of coherence between non-stationary signals (Lachaux et al., 1999).

Functional networks have largely been identified in task-based data by graph theory methods, where synchronized activity across different regions is thought to reflect intrinsic connectivity (Shafto and Tyler, 2014). Networks are formed from the wavelet coherence of multiple head electrode points and are thought to be functionally specialized by virtue of their interregional connectivity. Much of our understanding of brain connectivity rests on the way that it is measured and modeled. We consider a functional connective model approach: it has its basis in graph theory that aims to describe the network topology of (undirected) connections of the sort measured by noninvasive functional connectivity between remote sites. After brain network is constructed based on wavelet coherence, different time stages are divided during the stimuli process, the module is got by minimum spanning tree in every stage, and these are applied in dynamic programing in different states to construct the dynamic evolution model. The aim of the present study was to evaluate a possible correlation between the brain connectivity architecture and dynamic evolution processing as extracted from EEG recordings by dynamic model. EEG recording in the brain functional connectivity via wavelet coherence can be technically challenging. We aimed to assess the feasibility and the efficacy of auditory stimuli EEG (Lachaux et al., 2002).

2. Brain network construct and analysis

We discuss the cross wavelet transform and wavelet coherence for examining relationships in time–frequency space between two time series, brain network is constructed and analyzed based the wavelet coherence and graph theory, and minimum spanning tree method is used to module the brain regions, prepared to construct the dynamic model by dynamic programing algorithm.

Functional connectivity between brain regions is defined as the statistical dependence between neurophysiological signals in different brain areas and is typically determined by calculating the relationship between regional times series using wavelet coherence, The nodes of the network are EEG channels, and the edges of the network are weighed by the wavelet coherence values, a weighted graph is a mathematical representation of a set of elements (vertices) that may be linked through connections of variable weights (edges). In the present study, weighted and undirected networks were built. The vertices of the networks are the estimated cortical sources in the EEG, and the edges are weighted by the wavelet coherence within each pair of vertices. The undirected networks are constructed based on the threshold by the weighted Clustering coefficient C

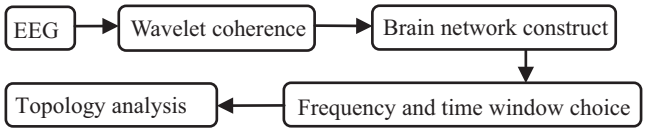

Figure 1 Schema of the brain network construction based on wavelet coherence.

and Weighted Characteristic Path length L, and module is got by minimum spanning tree. The process is as shown in Fig. 1.

2.1. Morlet wavelet transform and coherence

The wavelet transform can be launched with efficient frequency and time parameters. A wavelet theory, then, can be defined by Eqs. (1) and (2). Eq. (3) yields, then, W. Given a time series $f(t)$:

$$W_\psi f(a,b) = \frac{1}{\sqrt{|a|}} \int_{-\infty}^{+\infty} f(t)\psi * \left(\frac{t-b}{a}\right) \mathrm{d}t \tag{1}$$

$$\begin{aligned} W_f(a,b) &= \langle f(t), \psi_{a,b}(t)\rangle = \int_{-\infty}^{\infty} f(t), \psi^*_{a\cdot b}(t)\mathrm{d}t \\ &= \int_{-\infty}^{\infty} f(t)\frac{1}{\sqrt{a}}\psi^*\left(\frac{t-b}{a}\right)\mathrm{d}t \ \ (a>0, f\in L^2(R)) \end{aligned} \tag{2}$$

where $\psi_{a,b}(t) = \frac{1}{\sqrt{a}}\psi(\frac{t-b}{a})$

If $f(t) = f(k\Delta t)$, $t\in(k,k+1)$ then

$$\begin{aligned} W_f(a,b) &= \sum_k \int_k^{k+1} f(t)|a|^{-1/2}\psi^*\left(\frac{t-b}{a}\right)\mathrm{d}t \\ &= \sum_k \int_k^{k+1} f(k)|a|^{-1/2}\psi^*\left(\frac{t-b}{a}\right)\mathrm{d}t \\ &= |a|^{-1/2}\sum_k f(k)\left(\int_{-\infty}^{k+1}\psi^*\left(\frac{t-b}{a}\right)\mathrm{d}t - \int_{-\infty}^{k}\psi^*\left(\frac{t-b}{a}\right)\mathrm{d}t\right) \end{aligned} \tag{3}$$

where $a\in R$, $a\neq 0$. The parameter a controls the width of the wavelet and indicates the position of wavelet in frequency domain, and b controls the location of the wavelet and represents the position of wavelet in time domain. When using wavelets for feature extraction purposes, the Morlet wavelet (with $\omega_0 = 6$) is a good choice, since it provides a good balance between time and frequency localization (Faust et al., 2015; Samant et al., 2000; Ghorbanian et al., 2015).

$$\psi_0(\eta) = \pi e^{i\omega_0\eta} e^{-\eta^2/2} \tag{4}$$

where ω_0 is dimensionless frequency and η is dimensionless time. This expression shows that Morlet wavelet is a complex sine wave within a Gaussian envelope, which has the form of a Gaussian function centered at f_0, where f_0 determines the wave numbers within the envelope. Here $f_0 = 0.8125$, this gives a real part where the peaks next to the central peak are half the amplitude of the central peak.

In order to study the relationship between two non-stationary processes, definitions of cross spectrum and coherence are required. Given two processes x and y with their time–frequency representations wavelet power spectrum $W_x(a,b)$ and $W_y(a,b)$, the time–frequency cross spectrum between them is defined as wavelet power spectrum for WCS (Wavelet Cross Spectrum), and cross wavelet power spectrum are denoted by Eqs. (5),

$$WCS_{x,y}(a,b) = W_x(a,b)\cdot W^*_y(a,b) \tag{5}$$

It can be seen that the $WCS_{xy}(a,b)$ represents the time–frequency similarity of two signals x and y. Schwartz inequality guaranteed WC_{xy}(a,b) is between 0 and 1. 0 indicates that the corresponding time position of the two signals is independent, and the 1 represents the complete correlation.

Cross wavelet power reveals areas with high common power. Another useful measure is how coherent the cross wavelet transform is in time–frequency space. We define the wavelet coherence of two time series as,

$$WC_{xy}(a,b) = \frac{S(WCS_{xy}(a,b))}{\sqrt{S\left(|W_x(a,b)|^2\right)}\sqrt{S\left(|W_y(a,b)|^2\right)}} \tag{6}$$

The wavelet power, then, yields the squared absolute value of wavelet coefficients of x and y. The wavelet power spectrum and cross wavelet power spectrum, thus, represent the local variance of x (or y) and local covariance between x and y, respectively, through time and frequency. Therefore, one may depict complex wavelet coherency by Eq. (6).

Where scale denotes smoothing along the wavelet scale axis and S time smoothing in time. It is natural to design the smoothing operator so that it has a similar footprint as the wavelet used. Smoothing is achieved by removing high frequencies and retaining low frequencies. Notice that this definition closely resembles that of a traditional correlation coefficient, and it is useful to think of the wavelet coherence as a localized correlation coefficient in time–frequency space. For the Morlet wavelet a suitable smoothing operator is given by Torrence and Webster.

$$S_t(W_x(a,b)) = W_x(a,b) * c_1^{-\frac{t^2}{2a^2}} \tag{7}$$

$$S_a(W_x(a,b)) = W_x(a,b) * c_2\Pi(0.6a) \tag{8}$$

where c_1 and c_2 are normalization constants and Π is the rectangle function. The factor of 0.6 is the empirically determined scale decorrelation length for the Morlet wavelet .In practice both convolutions are done discretely and therefore the normalization coefficients are determined numerically.

The smoothing function S by Eqs. (6), (7) and (8).

$$S(W) = S_a[S_t(W)] \tag{9}$$

According to the above algorithm, the 1 s long EEG signals is respectively analyzed, as shown in the figure below (Fig. 2), firstly, the two signal segments of continuous wavelet coefficients is obtained (the horizontal axis is time, the unit is ms, the vertical axis for the wavelet coefficients can also be converted into the corresponding scale) and the second row is smoothing (the horizontal axis is time and the vertical axis is the smoothed spectrum value), finally, a two signal wavelet coherence value (the horizontal axis is time, Y-axis is the coherent value).

2.2. Topological character analysis and expression

2.2.1. Experiment

Auditory Stimuli were recorded by two adult (male and female, for eliminating the gender difference) native Chinese speakers. The congruent stimuli consisted of the word/Da/ (means loud voice) spoken loudly and the word/Xiao/(means low voice) spoken lowly. The incongruent stimuli consisted of the word /Da/spoken lowly and the word/Xiao/spoken

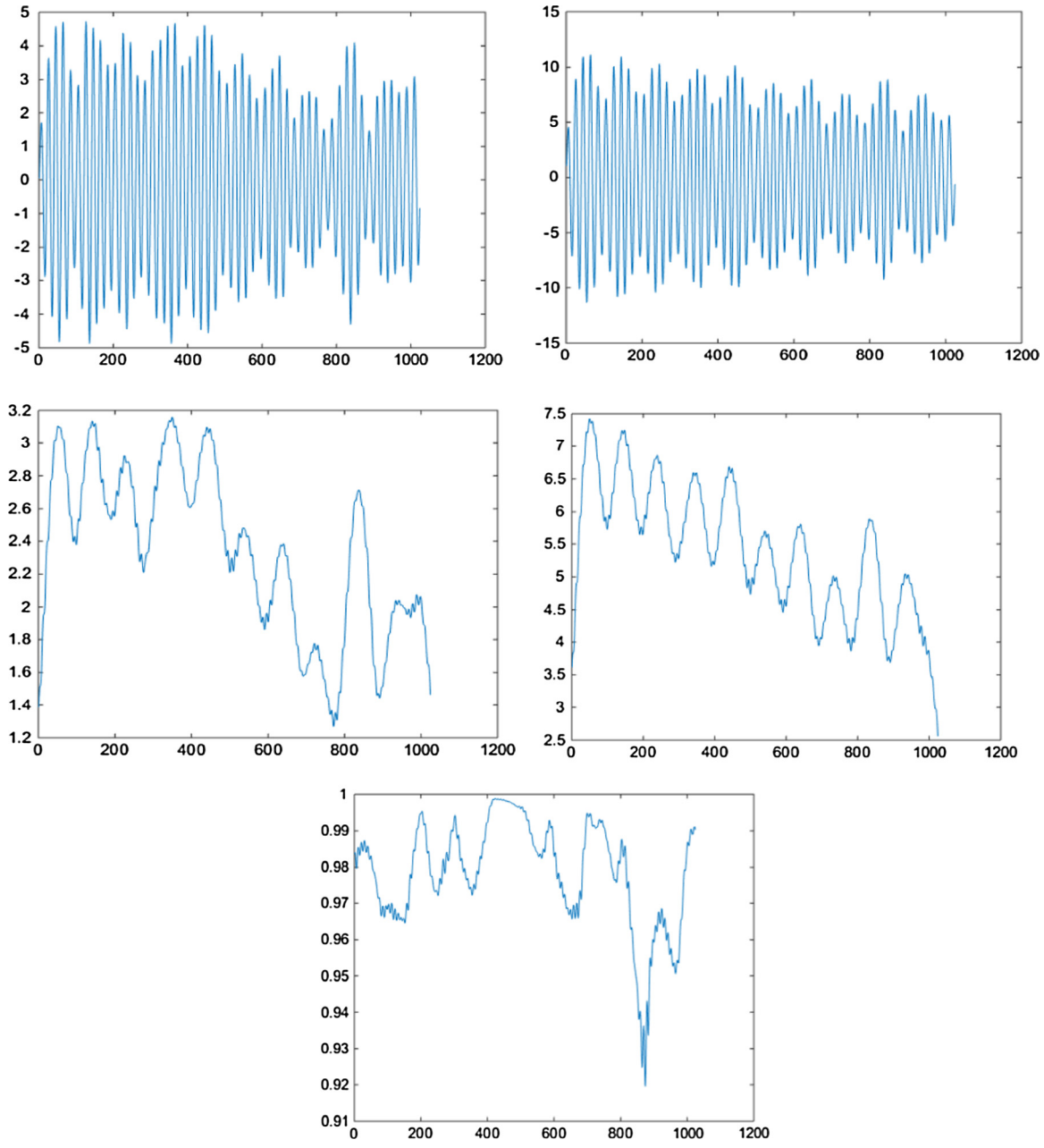

Figure 2 Wavelet coherence process.

loudly. Loudness difference between the low stimuli and the loud stimuli were adjusted at 30 dB. These two words have similar vowel and consonant duration (both of them are two-syllable words, and the cues of both words were located in the same character of the words), as well as similar appearance frequency in Chinese daily language. In the task, participants were instructed to identify the volume of the words and press the upper button (↑) for a loud volume or the lower button (↓) for a low volume, regardless of the meaning of the words. The task consisted of 320 trials. The four kinds of stimuli were randomly presented with equal probability (0.25) by the audio amplifier, which is limited to less than 60 db. The duration of every auditory stimulus was 400 ms, and the interval between every two stimuli was 2000, 2100, 2200, 2300 or 2400 ms.

2.2.2. Topologic character analysis

The following figure (Fig. 3 right) is the normalization of the average shortest path length and clustering coefficient in the word /Da/ (means loud voice) spoken loudly. Brain networks have small world properties of high clustering coefficient and a short average shortest path length. So the wavelet coherence threshold is 0.64 in Fig. 3 (right, The X axis represents the normalization path length and clustering coefficient, the Y axis represents the wavelet coherence threshold, generating binary network.) EEG recordings are into distinct frequency bands, namely delta (0.5–4 Hz), theta (4–8 Hz), alpha (8–13 Hz), beta (13–30 Hz) and gamma (30–90 Hz). Furthermore, each frequency band is associated with distinct cognitive functions. So the thick lines represent alpha band is significantly different in Fig. 3 (left, The Y axis represents the path length and the X

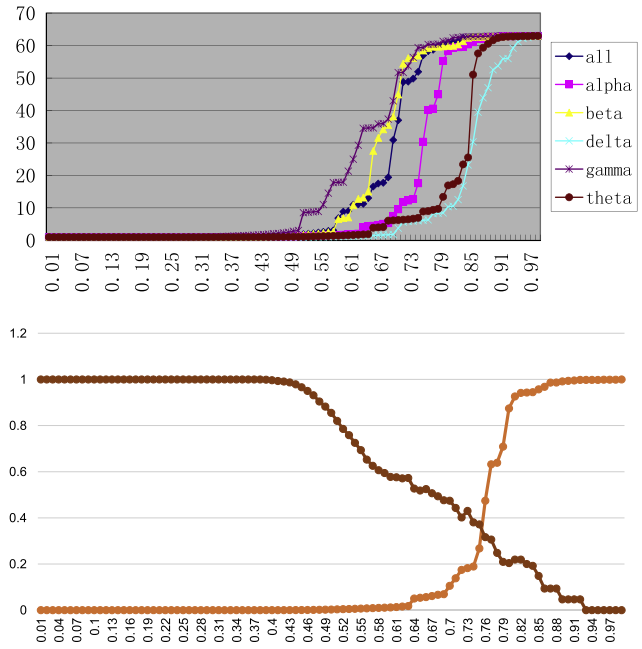

Figure 3 The characteristic path length in difference frequency (left), the normalization of the alpha average shortest path length and clustering coefficient in/Da/spoken loudly (right).

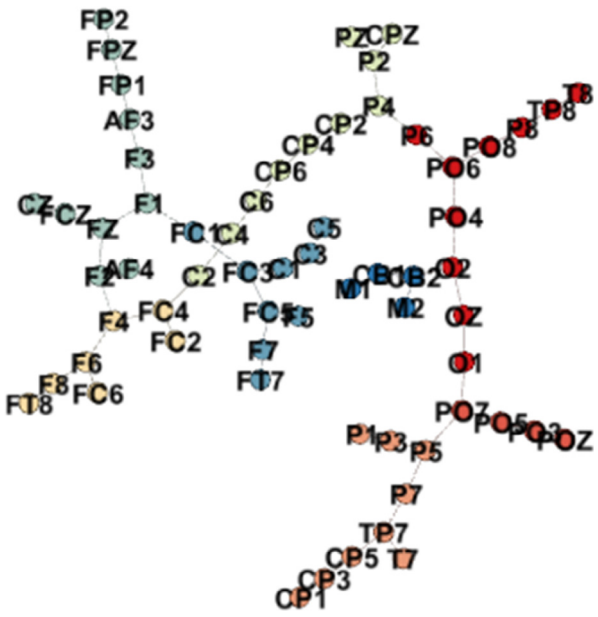

Figure 4 Brain module partition based on minimum spanning tree method.

axis represents the wavelet coherence threshold), so the alpha frequency analysis is choice firstly (Deco and Kringelbach, 2014; Vecchio et al., 2016).

2.2.3. The minimum spanning tree

The minimum spanning tree (MST) of a weighted graph connects all the given data points at the lowest possible cost, so the reciprocal of wavelet coherence is used to compute the minimum spanning tree by Kruskal algorithm. If the weights of the edges represent the distances between the data points, removing edges from the MST leads to a collection of connected components which can be defined to be clusters. The data must have well-separable clusters in order that they can be recognized with the MST clustering. On the other hand, the method does not need any parameters like the number of clusters or some other a priori information about the underlying data. Highly connected vertices can be thought to be "cluster centers", in this paper, the maximum degree is used to choose the cluster and centers, for example, the different cluster is in different colors as shown in Fig. 4 (Päivinen, 2005; Onnela et al., 2005).

2.3. The dynamic model construct

We used functional EEG and dynamic evolution modeling to firstly investigate the cortical dynamics among the region. The brain activation of the intelligibility effect and the effective connectivity among the brain regions were analyzed for both language groups under identical procedures and then put together for comparison. Deciding on the most appropriate connectivity measure can be arduous, as several issues should be considered. This includes the consideration of linear or nonlinear relations, analysis in time or frequency domain, using an amplitude or phase-based measure, obtaining directed or undirected information, wavelet coherence is to investigate connectivity of the brain, which has been used for several decades and are relatively straightforward in terms of computation and interpretation in Fig. 5. Functional networks are based on the strength or consistency of functional interactions between the network nodes. So the degree is chosen to represent the dynamic evolution parameter.

The brain network construction is based on wavelet coherence analysis, as shown quantitatively in Fig. 2. The time horizon is sampled into T discrete stages that are equally spaced along the length of the driving cycle. Sliding-window is 30 ms from −100 ms to 600 ms. The vertical axis is quantized into S different states (64 channel in this paper). There are many clusters in a stage. In graph theory, the degree of a vertex is the number of edges incident to the vertex, every vertex presents the degree value in every stage and every channel.

The state vector u is composed of degree levels that range in equal steps. The paper deals with degree of node and battery to maximize the cost function. For this reason, the node and the degree can be considered as the state vector. By fixing one, the other can be derived from the degree balance equation, hence the degree is natural to program. In this case, Fig. 6, reveals a model of the network along with all interconnected nodes. The total number of nodes is S_T which depends on the number of selected states and time samples. Each of these nodes (N) is indexed according to its current stage location and corresponding state. For example node N_{iu_j} corresponds to the node at stage i and state u_j. At the first stage each node is characterized with a cost function D_{iu_j} symbol as nodal cost. This is a discrete closed form function that defines a certain objective. The nodal cost represents the cost of being in the associated state. Starting the second stage until ¼ T, each node has two associated costs which are the nodal cost and the transition cost. The transition cost R_{u_k,iu_j} is the cost of moving from

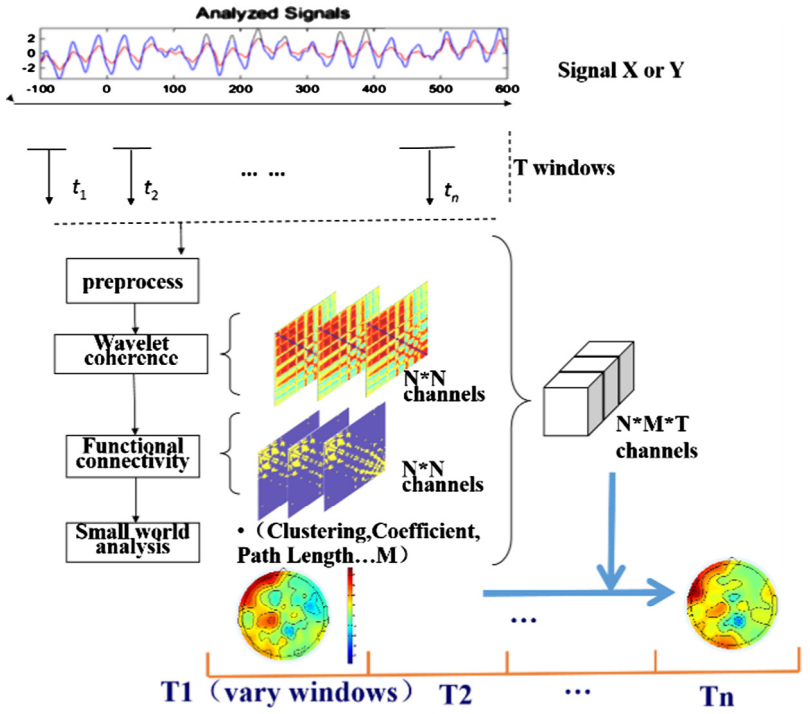

Figure 5 Functional connectivity dynamics analysis model.

the previous states u_k to the current state u_j at i. The total cost $F_i u_j$ associated with each node at a certain stage is the sum of its nodal cost and the maximum value of all transition costs to the node from previous stage as shown in Eq. (10) and this processing is in algorithm 1 (Fares et al., 2015), C_{iu_j} is the cluster which is cognition brain areas according to the D_{iu_j}. Therefore, the dynamic evolution is expressed during the stimuli.

$$\text{Index}\begin{cases}\text{State Vector}: u=[u_1\ u_2\ldots u_j\ldots u_s]\ j=1:\text{S}\\ \text{Stage Vector}:\ \text{Stage}=[1\ 2\ldots i\ldots \text{T}]\ i=1:\text{T}\\ \text{Node Representation}:\ \text{N}_{iu_j}\\ \text{Node Cost}: \text{D}_{iu_j}\\ \text{Cluster}: \text{C}_{iu_j}\\ \text{Transition Cost}: \text{R}_{u_k,iu_j}\ \ k=1:S\end{cases} \tag{10}$$

Algorithm 1 dynamic evolution Algorithm

```
for such that i = 1:T do
  for such that j = 1:S do
    for such that k = 1:S do
      Compute D_{iu_j}
      Compute R_{u_k,iu_j} ∀k
      Compute C_{iu_j}
      Locate maximum of R_{u_k,iu_j}, Locate C_{iu_j}
      Save index of Max = [i, k_max] for max of R_{u_k,iu_j}
      Compute F_{iu_j} = D_{iu_j} + R_{u_k,iu_j} + D_{(i-1)u_k}
    end for
  end for
end for
```

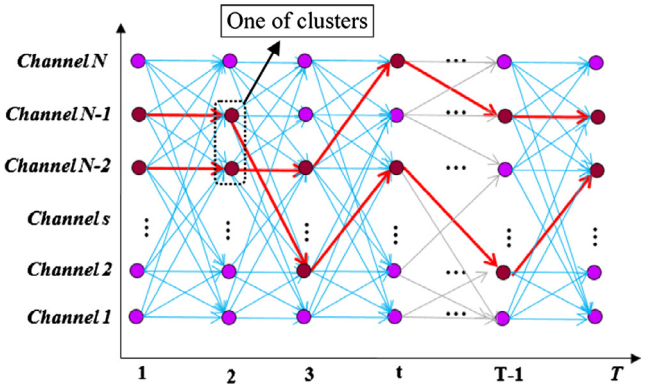

Figure 6 Dynamic evolution sketch.

2.4. Result

The dynamic evolution processing mapping is presented in Fig. 7 based on node degrees in binary network in incongruent minus congruent in alpha frequency. Moreover, our further research is to study brain oscillation mechanisms of auditory cognitive control processing based on the dynamic evolution model. We found that the different auditory stimuli arouse different brain areas. This finding provides evidence for an auditory conflict processing signal. More specifically, we proposed a new model to investigate the different cognition processing in Fig. 7 that corresponds to Fig. 8 in 30 ms time windows. High wavelet coherence represents high synchronization of neurons, the dynamic evolution processing mapping (incongruent minus congruent) is that the bigger node degree the greater the color is depth. It can be seen that the degree of synchronization in

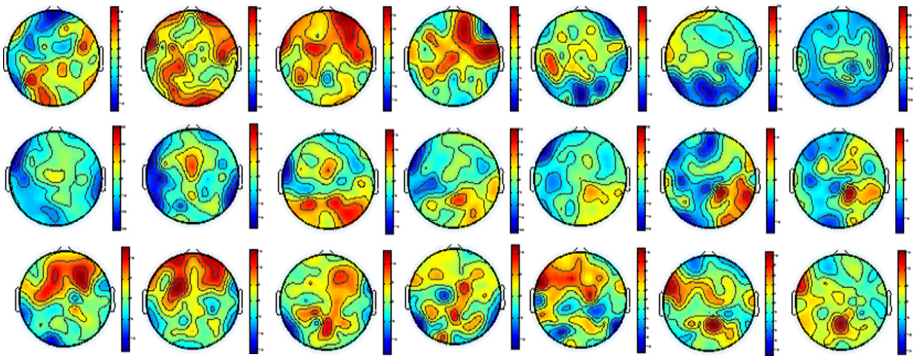

Figure 7 The dynamic evolution processing mapping (incongruent minus congruent).

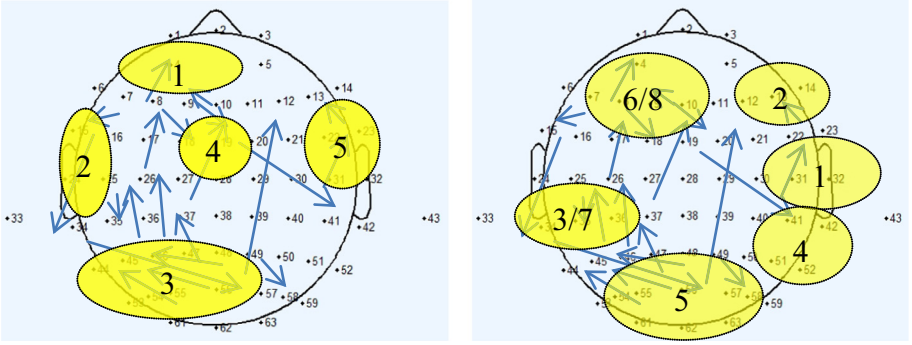

Figure 8 The dynamic evolution processing in different auditory input.

the former stage, the front right brain area synchronization is higher than other areas. At the later stage, the middle frontal brain area in incongruent is higher than other areas. The results are consistent with auditory cognitive control.

Moreover, the stronger forward connections between the anterior temporal poles and Broca's area may be due to further semantic processing that is included in word identification through phonological information in Chinese in Fig. 8 (left: word/da/spoken loudly and right: word/Xiao/spoken loudly). It can be seen in the process of auditory cognitive control, the high synchronization brain areas change in time and area. This preliminary result for auditory Stroop suggests an integrated forward processing of mapping the phonological information to the semantic-related representation from both hemispheres in this tonal language. In an auditory Stroop task, participants are typically required to respond to the acoustic properties of speech stimuli, and ignore the word meanings (Yu et al., 2015). Results: All subjects showed that most of the activation areas were on the Dorsal lateral prefrontal cortex (DLPFC) as shown in Fig. 8 in accordance with human's cognition (Zhang et al., 2013).

3. Conclusion

The model indicates that a complete cognitive control process is perceptual detection, identification detection, and conflict resolution during the auditory Stroop task. Understanding the role EEG oscillations is important for comprehending mechanisms of cognitive decline in the network dynamics of auditory stimuli and could serve as a model for understanding large-scale brain network dynamics and their relation to other cognitive phenomena or structural modulations. This study opens interesting avenues into future researches investigating eventual modifications of brain connectivity in the evolution of neurodegenerative processes beginning at the very early, pre-clinical stages. Node degree is used to construct the model in this paper, in the future, more topological parameters are considered to build the model. There are still a few details that need ironing out, for example, the length of the time window, dynamic programing algorithm optimization (Fares et al., 2015), etc. In brief, such methodologies will be suitable for capturing the dynamic evolution of the time varying connectivity patterns that reflect certain cognitive tasks or brain pathologies.

Acknowledgements

Our thanks to supports from the National Natural Science Foundation of China (61171186, 61271345, 61671187), Key Laboratory Opening Funding of MOE-Microsoft Key Laboratory of Natural Language Processing and Speech (HIT.KLOF.20150xx, HIT.KLOF.20160xx), Shenzhen science and technology project (JCYJ20150929143955341), and the Fundamental Research Funds for the Central Universities (HIT.NSRIF.2012047). Heilongjiang Provincial Department of Education Science and Technology Research Project (12533051), The Project of young talents of Heilongjiang University of Science and Technology of China in 2013 (NO. Q20130106).

References

Bonato, P., Gagliati, G., Knaflitz, M., 1996. Analysis of myoelectric signals recorded during dynamic contractions. IEEE Eng. Med. Biol. Mag. 15 (6), 102–111.

Deco, G., Kringelbach, M.L., 2014. Great expectations: using whole-brain computational connectomics for understanding neuropsychiatric disorders. Neuron 84 (5), 892–905.

Fares, D., Chedid, R., Panik, F., Karaki, S., Jabr, R., 2015. Dynamic programming technique for optimizing fuel cell hybrid vehicles. Int. J. Hydrogen Energy 40 (24), 7777–7790.

Faust, O., Acharya, U.R., Adeli, H., Adeli, A., 2015. Wavelet-based eeg processing for computer-aided seizure detection and epilepsy diagnosis. Seizure 26, 56–64.

Ghorbanian, P., Devilbiss, D.M., Hess, T., Bernstein, A., Simon, A.J., Ashrafiuon, H., 2015. Exploration of eeg features of alzheimer's disease using continuous wavelet transform. Med. Biol. Eng. Comput. 53 (9), 1–13.

Kopal, J., Burian, J., 2014. Complex continuous wavelet coherence for eeg microstates detection in insight and calm meditation. Conscious. Cogn. 30 (3), 13–23.

Lachaux, J., Rodriguez, E., Martinerie, J., Varela, F.J., 1999. Measuring phase synchrony in brain signals. Hum. Brain Mapp. 8 (4), 194–208.

Lachaux, J.P., Rodriguez, E., Martinerie, J., Adam, C., Hasboun, D., Varela, F.J., 2000. A quantitative study of gamma-band activity in human intracranial recordings triggered by visual stimuli. Eur. J. Neurosci. 12 (7), 2608–2622.

Lachaux, J.P., Lutz, A., Rudrauf, D., Cosmelli, D., Le, V.Q.M., Martinerie, J., et al, 2002. Estimating the time-course of coherence between single-trial brain signals: an introduction to wavelet coherence. Neurophysiol. Clin. 32 (3), 157–174.

Milligen, B.P.V., Sánchez, E., Estrada, T., Hidalgo, C., Brañas, B., Carreras, B., et al, 1995. Wavelet bicoherence. a new turbulence analysis tool. Phys. Plasmas 2 (8), 3017–3032. 1994-present.

Nagai, Y., Critchley, H.D., Featherstone, E., Fenwick, P.B.C., Trimble, M.R., Dolan, R.J., 2004. Brain activity relating to the contingent negative variation: an fmri investigation. Neuroimage 21 (4), 1232–1241.

Onnela, J.-P., Saramäki, J., Kertész, J., Kaski, K., 2005. Intensity and coherence of motifs in weighted complex networks. Phys. Rev. E: Stat., Nonlin. Soft Matter Phys. 71 (2), 531–536.

Osofsky, S.S., 2000. Calculation of transient sinusoidal signal amplitudes using the morlet wavelet. IEEE Trans. Signal Process. 47 (12), 3426–3428.

Päivinen, N., 2005. Clustering with a minimum spanning tree of scale-free-like structure. Pattern Recogn. Lett. 26 (7), 921–930.

Samant, A., Adeli, H., 2000. Feature extraction for traffic incident detection using wavelet transform and linear discriminant analysis. Comput.-Aided Civ. Infrastruct. Eng. 15 (4), 241–250.

Santoso, S., Powers, E.J., Bengtson, R.D., Ouroua, A., 1997. Time-series analysis of nonstationary plasma fluctuations using wavelet transforms. Rev. Sci. Instrum. 68 (1), 898–901.

Shafto, M.A., Tyler, L.K., 2014. Language in the aging brain: the network dynamics of cognitive decline and preservation. Science 346 (6209), 583–587.

Sporns, O., 2011. Networks of the Brain. MIT Press.

Torrence, C., Compo, G.P., 1998. A practical guide to wavelet analysis. Bull. Am. Meteorol. Soc. 79 (79), 61–78.

Vecchio, F., Miraglia, F., Piludu, F., Granata, G., Romanello, R., Caulo, M., et al, 2016. "Small world" architecture in brain connectivity and hippocampal volume in alzheimer's disease: a study via graph theory from eeg data. Brain Imaging Behav., 1–13

Vincent, J.L., Snyder, A.Z., Fox, M.D., Shannon, B.J., Andrews, J.R., Raichle, M.E., et al, 2006. Coherent spontaneous activity identifies a hippocampal-parietal memory network. J. Neurophysiol. 96 (6), 3517–3531.

Yu, B., Wang, X., Ma, L., Li, L., Li, H., 2015. The complex pre-execution stage of auditory cognitive control: erps evidence from stroop tasks. PLoS One 10 (9), e0137649.

Zhang, G., Yao, L., Zhang, H., Long, Z., Zhao, X., 2013. Improved working memory performance through self-regulation of dorsal lateral prefrontal cortex activation using real-time fmri. PLoS One 8 (8), 843.